Published in final edited form as:
Am J Transplant. 2008 December ; 8(12): 2516–2526. doi:10.1111/j.1600-6143.2008.02444.x.

Rejection of Cardiac Xenografts Transplanted from α 1,3-Galactosyltransferase Gene-Knockout (GalT-KO) Pigs to Baboons

Y. Hisashi[a], **K. Yamada**[a], **K. Kuwaki**[a], **Y.-L Tseng**[a], **F. J. M. F. Dor**[a], **S. L Houser**[b], **S. C. Robson**[c], **H.-J. Schuurman**[d], **D. K. C. Cooper**[a], **D. H. Sachs**[a], **R. B. Colvin**[b], and **A. Shimizu**[a,b,d,e,*]

[a] Transplantation Biology Research Center, Massachusetts General Hospital/Harvard Medical School, Boston, MA

[b] Department of Pathology, Massachusetts General Hospital/Harvard Medical School, Boston, MA

[c] Department of Medicine, Transplant Center, Beth Israel Deaconess Medical Center/Harvard Medical School, Boston, MA

[d] Immerge BioTherapeutics Inc., Cambridge, MA

[e] Department of Pathology, Nippon Medical School, Tokyo, Japan

Abstract

The use of α 1,3-galactosyltransferase gene-knockout (GalT-KO) swine donors in discordant xenotransplantation has extended the survival of cardiac xenografts in baboons following transplantation. Eight baboons received heterotopic cardiac xenografts from GalT-KO swine and were treated with a chronic immunosuppressive regimen. The pathologic features of acute humoral xenograft rejection (AHXR), acute cellular xenograft rejection (ACXR) and chronic rejection were assessed in the grafts. No hyperacute rejection developed and one graft survived up to 6 months after transplantation. However, all GalT-KO heart grafts underwent graft failure with AHXR, ACXR and/or chronic rejection. AHXR was characterized by interstitial hemorrhage and multiple thrombi in vessels of various sizes. ACXR was characterized by TUNEL$^+$ graft cell injury with the infiltration of T cells (including CD3 and TIA-1$^+$ cytotoxic T cells), CD4$^+$ cells, CD8$^+$ cells, macrophages and a small number of B and NK cells. Chronic xenograft vasculopathy, a manifestation of chronic rejection, was characterized by arterial intimal thickening with TUNEL$^+$ dead cells, antibody and complement deposition, and/or cytotoxic T-cell infiltration. In conclusion, despite the absence of the Gal epitope, acute and chronic antibody and cell-mediated rejection developed in grafts, maintained by chronic immunosupression, presumably due to *de novo* responses to non-Gal antigens.

Keywords

Acute rejection; baboon; cellular rejection; chronic rejection; humoral rejection; xenotransplantation

*Corresponding author: Akira Shimizu, Akira.Shimizu@tbrc.mgh.Harvard.edu.

Introduction

Transplantation has become the preferred therapy for the treatment of end-stage heart disease, but its applicability has been limited by deceased donor shortages. Hearts derived from animals could alleviate the critical shortage of organs available for clinical transplantation (1–3). The pig is the current animal of choice for clinical xenotransplantation because of its size, physiologic compatibility, breeding characteristics and the potential for genetic modification (1–3). When pig organs are transplanted into primates, however, they are rapidly rejected by hyperacute rejection (HAR) and acute humoral xenograft rejection (AHXR), also known as acute vascular rejection or delayed xenograft rejection (4–8). Both HAR and AHXR are triggered by xenoreactive natural antibodies, which are directed against the galactose α 1,3-galactose (Gal) epitope on porcine vascular endothelium (6–8).

In a recent attempt to prevent HAR and AHXR, α 1,3-galactosyltransferase gene-knockout (GalT-KO) pigs that do not express the Gal epitope were produced (9,10). We reported our initial study of cardiac transplantation from GalT-KO miniature swine to baboons that were treated with a chronic immunosuppressive regimen (11,12). No grafts in this study succumbed to HAR, and the grafts survived consistently longer than grafts from previous studies using miniature swine or human decay-accelerating factor (hDAF) transgenic pigs as donors (13–15).

The rejection of allografts by acute humoral, cellular and chronic rejection has been well characterized (16). However, few studies of cell-mediated rejection (acute cellular xenograft rejection: ACXR) or chronic rejection in discordant xenografts have been reported, as almost all such grafts are rejected primarily by AHXR. In our initial study of GalT-KO heart xenotransplantation, cellular infiltration occurred along with AHXR in all eight grafts. Furthermore, chronic rejection, as characterized by chronic xenograft vasculopathy, developed in three of the long-term surviving cardiac xenografts. In this study, we characterized the pathology of the GalT-KO cardiac xenografts in baboons in order to clarify the process by which graft failure develops and to characterize the pathology of AHXR, as well as acute cellular and chronic xenograft rejection.

Materials and Methods

Animals

Eight heterotopic heart transplantations were performed in baboons *(Papio hamadryas;* Manheimer Foundation, Homestead, FL) of body weight 9–22 kg, using GalT-KO miniature swine of body weight 9–27 kg as donors (11,12). All GalT-KO donors were individually generated by nuclear transfer from GalT-KO fibroblasts from Massachusetts General Hospital (MGH) major histocompatibility complex (MHC)-inbred miniature swine (10). All animal care procedures were performed in accordance with the *Principles of Laboratory Animal Care* formulated by the National Society for Medical Research and the *Guide for the Care and Use of Laboratory Animals* prepared by the Institute of Laboratory Animal Resources and published by the National Institutes of Health (NIH publication no. 86–23, revised 1996). All protocols were approved by the MGH Subcommittee on Research Animal Care.

Transplantation and immunosuppression

The surgical procedures associated with heterotopic (intra-abdominal) heart transplantation in baboons, and the immunosuppressive treatment, supportive therapy and monitoring of recipient baboons have been previously described in detail (11,12). The chronic immunosuppressive regimen for these baboons included an induction treatment of horse antihuman thymocyte globulin (ATGAM; Upjohn, Kalamazoo, Ml) 50 mg/kg/day i.v. on

days −3, −2 and −1. Thymic irradiation (700 cGy) was given on day −1 except in one baboon (B228). Complement was depleted in five out of eight baboons by cobra venom factor (CVF) for either 4 days (B226, B228, B229) or 14 days (B214, B216). Maintenance therapy consisted of a human antihuman CD154 monoclonal antibody (mAb) (ABI793, generously provided by Novartis Pharma AG, Basel, Switzerland) administered i.v. at 25 mg/kg on days −1, 0, 1, 4, 7, 10 and 14, followed by 20 or 25 mg/kg every 5 days thereafter; mycophenolate mofetil (MMF) that was administered by continuous i.v. infusion from day −2 to maintain a whole blood level of 3–5 μg/mL and methylprednisolone that was given from day 0 (2 mg/kg × 2 i.v. daily for 7 days, followed by tapering to 0.5 mg/kg i.v. daily over the next 35 days). MMF in B223 was significantly reduced, beginning on day 59. Heparin (3–60 U/kg/h) was started as anticoagulant therapy on the day of transplantation and was titrated to maintain a partial thromboplastin time (PTT) of 150 s. Three baboons (B223, B225, B229) received recombinant antithrombin (750 U/kg/day, generously provided by GTC Biotherapeutics, Framingham, MA) from days 1–12 and were therefore given alternative heparin regimens. These animals were maintained on low-dose heparin (B225), given lowdose heparin only on days 0 and from day 13 to the end of the experiment (B223), or maintained at maximum dose (PTT 150 s) beginning on day 7 (B229). In these cases, the levels of antithrombin were at least in the high normal range. Three baboons were treated with aspirin (40 mg given p.o. every other day), beginning on days 4 (B228), 16 (B229) or 75 (B223). Graft function was monitored by measuring graft palpation scores (grade 3 representing excellent graft contractions and grade 0 representing cessation of contractions) and serum troponin T levels (11,12).

Histological and immunohistochemical examination

Heart graft samples were taken from open needle biopsies and from graftectomies (Table 1). For light microscopic examination, tissue was fixed in 10% buffered formalin and embedded in paraffin. Sections were examined after hematoxylin and eosin (H&E) and Elastica Masson Goldner (EMG) staining. Tissues for electron microscopy were fixed in 2.5% glutaraldehyde + 2% paraformaldehyde, postfixed with 1% osmium tetroxide and embedded in Epon 812. Ultrathin sections were stained with lead citrate. Frozen tissue sections were stained by the direct immunofluorescent technique, using a fluorescein isothiocyanate (FITC)-conjugated rabbit polyclonal antibody to human IgG, IgM, C3 and fibrinogen (all from DAKO, Carpinteria, CA), and the indirect immunofluorescent technique, using an antihuman C4d mAb (Quidel, San Diego, CA), polyclonal rabbit antihuman C4d antibody (American Research Products, Inc., Belmont, MA) and antihuman C5b-9 mAb (DAKO). The following primary antibodies were used in staining by the standard avidin–biotin–peroxidase complex (ABC) technique (17): (1) anti-TIA-1 mAb (GMP-17, granule membrane protein of 17 kDa; Coulter Immunology, Hialeah, FL), which detects cytotoxic granule protein in T and NK cells; (2) antihuman α-smooth muscle actin mAb (αSMA, 1 A4; DAKO), which detects smooth muscle cells in arteries; (3) polyclonal rabbit antihuman CD3 antibody (A0452; DAKO), antihuman CD4 mAb (1 F6; Nitirei, Tokyo, Japan), antihuman CD8 mAb (C8/144 B; Nitirei), antihuman CD20 mAb (B cells, L26; DAKO), antihuman CD68 mAb (macrophages, KP-1, DAKO), antihuman NKB1 mAb (NK cells, DX9; BD Biosciences, San Jose, CA) and antihuman CD56 mAb (NCAM/NK cells, 1 B6; Nitirei) were used to examine the phenotype of infiltrating cells. To detect cytotoxic T cells in xenografts, two-color immunohistochemistry staining against TIA-1 (alkaline phosphatase, blue color) and CD3 (DAB, brown color) was performed. The relationship between $CD41^+$ platelet thrombi and the deposition of immunoglobulin and complement was assessed using two-color immunohistochemistry for CD41 (Texas Red) and C4 d (FITC). In histological sections, fragmented nuclear DNA associated with apoptosis was labeled by the terminal deoxynucleotidyl transferase (TdT)-mediated dUTP-biotin nick end-labeling (TUNEL) method (18).

Quantification of histological Findings

The deposits of immunoglobulin (IgM and IgG) and complement (C3, C4 d and C5 b-9) and the frequency of microthrombi (EMG stain) were semi-quantified from (−) to (3+) dependent on their distribution and the intensity of the associated staining. In each graft sample, 40 randomly selected fields (at 400x, using an optical grid area of 0.0625 mm^2) were assessed without prior knowledge of the clinical or histological findings, and the mean semiquantitative staining score or the mean number of cells per single field for the following values was determined: (1) the number of $TUNEL^+$ cells in capillaries; (2) the number of $CD3^+$, $CD68^+$, $CD20^+$, $CD4^+$, $CD8^+$ and $NKB\text{-}1^+$ cells and (3) the presence of chronic xenograft vasculopathy in arterial cross-sections in all fields of the graftectomy samples and the percentage of arteries affected. In addition, in all arteries that were affected by chronic xenograft vasculopathy, vessel wall thickening was scored as 0 (normal artery), 1 (<10% occlusion), 2 (10–50% occlusion) or 3(>50% luminal occlusion) (19). Correlations between the numbers of $CD3^+$ cells and $TUNEL^+$ cells in capillaries and the interstitium were computed and analyzed using Pearson's test.

Results

Clinical course of GalT-KO heart grafts

Eight cardiac xenografts from GalT-KO swine were transplanted heterotopially to baboons treated with chronic immunosuppression. HAR did not develop in any of the GalT-KO grafts. However, AHXR gradually developed in all grafts.

The graft contraction and serum troponin T levels in baboons were assessed, as shown in Figure 1. Based on these parameters, the eight cardiac grafts were divided into three groups: (1) healthy-graft group: B226, B225 and B216 were euthanized, or died on days 16, 23 and 56 days posttransplantation, with cardiac grafts that were beating well and with stable or somewhat increased serum troponin T levels. These animals were sacrificed for reasons other than the rejection of the cardiac graft, namely the development of anemia (hematocrit <15%) at a time when donor blood was not available, an ischemic leg (associated with an indwelling femoral catheter) or spontaneous abdominal bleeding. (2) Rapidly weakened group: contractions in the grafts in B214 and B218 were stable and then rapidly weakened and ceased 59 and 67 days after transplantation, with a significant increase in recipient serum troponin T levels. (3) Gradually weakened group: in B229, B223 and B228, graft beating gradually weakened and then stopped 78, 110 and 179 days after transplantation, with or without increased recipient serum troponin T levels.

Pathology of grafts in healthy-graft, rapidly weakened and gradually weakened groups

In the cardiac grafts of the healthy-graft group, early AHXR occurred with focal interstitial hemorrhage and a few multiple microthrombi in the microvasculature (Figure 2A). Polymorphonuclear leukocytes and mononuclear cells infiltrated the grafts (Figure 2B). In the rapidly weakened group, advanced AHXR developed 59 and 67 days posttransplantation with an irregular distribution of interstitial hemorrhage and diffuse and multiple microthrombi in both the microvasculature and arteries (Figure 2C). Polymorphonuclear leukocytes were found within the grafts, as were infiltrating mononuclear cells (Figure 2D). Chronic xenograft vasculopathy was not detected in the grafts. In the grafts of the gradually weakened group, AHXR, ACXR and chronic xenograft vasculopathy developed 78 (B229), 110 (B223) and 179 (B228) days posttransplantation. Multiple microthrombi, located mainly within the microvasculature, were present along with focal interstitial hemorrhage (Figure 2E–G). A multifocal infiltrate of mononuclear cells was noted and was associated with myocyte damage (Figure 2H–J).

Acute humoral xenograft rejection (AHXR)

AHXR in GalT-KO heart grafts was characterized by the development of thrombotic microangiopathy and focal interstitial hemorrhage that was associated with immunoglobulin and complement deposition and subsequent capillary injury. A few multiple microthrombi were evident in the grafts of the healthy-graft group (Figure 2A). The grafts of the rapidly weakened group contained prominent multiple thrombi in both capillaries and arteries (Figure 2C). In contrast, in the grafts of the gradually weakened group, prominent multiple thrombi developed mainly within the microvasculature (Figure 2K–M). Deposits of immunoglobulin and complement were detected on capillaries and arteries in these grafts (Figure 2N and O). During the initial period after transplantation, IgM was clearly positive and IgG was weakly positive or negative (Table 1). As thrombotic microangiopathy developed, however, the increased frequency of microthrombi was paralleled by an increased frequency of IgM, IgG, C3, C4d and C5b-9 deposits (Table 1). Two-color immunohistochemistry for CD41 and C4d showed that almost all of the $CD41^+$ thrombi were detected within vessels with depositions of complement (Figure 2P). Electron microscopy revealed the loss of endothelial cells within these damaged capillaries, along with fibrin thrombi, interstitial hemorrhage and the destruction of capillary structure (Figure 2Q and R). AHXR in the grafts was also characterized by fibrinoid necrosis of arteries with immunoglobulin and complement deposition, neutrophil infiltration, the presence of $TUNEL^+$ dead cells and thrombus within the arteries (Figure 3A–H).

Acute cellular xenograft rejection (ACXR)

Early after transplantation, polymorphonuclear leukocytes and mononuclear cells infiltrated the grafts. In all biopsies from day 7 (the healthy-graft and rapidly weakened groups), the cellular infiltrate was composed of polymorphonuclear leukocytes and $CD68^+$ macrophages, as well as a small number of $CD3^+$ T cells (Figure 4A–D). In the graftectomy samples of the healthy-graft group by day 56, both polymorphonuclear leukocytes and mononuclear cells (polymorphonuclear leukocytes rather than mononuclear cells) infiltrated (Figure 4E and F). However, there were no mononuclear cell infiltrate foci that were clearly associated with myocyte damage. Therefore, according to the International Society for Heart and Lung Transplantation (ISHLT) standardized cardiac biopsy grading system (16), the acute cellular rejection grading in the healthy-graft group was grade OR. In all grafts after transplantation, the number of infiltrating cells increased (Figure 5). Although all biopsy samples showed ISHLT grade OR, analysis of graftectomy samples from the rapidly and gradually weakened groups revealed ISHLT grade 2R rejection (Figure 4G–T). Mononuclear cells were found within capillaries and extended into the surrounding interstitium. The infiltrating cells included $CD3^+$ T cells and $CD68^+$ macrophages, as well as a small number of $CD20^+$ B cells. Similar numbers of $CD4^+$ and $CD8^+$ T cells infiltrated the grafts. Two-color immunohistochemistry revealed $TIA\text{-}1^+$ cytotoxic granules in many infiltrating $CD3^+$ T cells, indicating that they were cytotoxic T cells. A small number of $NKB\text{-}1^+$ and $CD56^+$ NK cells infiltrated the grafts. $TUNEL^+$ dead cells were detected in contact with infiltrating mononuclear cells (Figure 4J and K). Microthrombi were occasionally found in regions of $CD3^+$ T-cell infiltration without AHXR-associated polymorphonuclear leukocytes and macrophage infiltration (Figure 4L). Furthermore, there was a weak, but significant correlation ($p < 0.05$) between the numbers of $CD3^+$ T cells and $TUNEL^+$ dead cells in the capillaries and interstitium (Figure 5). Acute endothelialitis was also seen in arteries in the graftectomy samples from the gradually weakened group (Figure 3I–L).

Chronic xenograft vasculopathy

As in cardiac allotransplantation, chronic xenograft vasculopathy is considered to be a feature of chronic rejection in xenotransplantation. In graftectomy samples from the gradually and rapidly weakened groups, fibrinoid necrosis and/or active endothelialitis were

seen in arteries associated with irregular thickening of arterial intima (Figure 3D and L). Furthermore, graftectomy samples from the gradually weakened group revealed typical chronic xenograft vasculopathy in arteries, which was characterized morphologically by the narrowing of arteries as a result of a thickening of the neointima with α-smooth muscle actin$^+$ cells (Figure 6). As in chronic allograft vasculopathy (CAV), elastosis failed to develop in the thickened neointima. Although the percentage of chronic xenograft vasculopathy was similar in both small intramural and large pericardial arteries, small arteries were generally more severely affected.

Histological characterization allowed us to differentiate four types of chronic xenograft vasculopathy. The first type, chronic humoral rejection-associated vasculopathy (Figure 7A–H), was characterized by arterial intimal thickening with the presence of TUNEL$^+$ cells and deposits of fibrin, immunoglobulin (IgM and IgG) and complement (C3, C4d and C5b-9). The second type, chronic cellular rejection-associated vasculopathy (Figure 7I–P), was characterized by mononuclear cell infiltration in the neointima, with active endothelialitis and TUNEL$^+$ cells. The cellular infiltration in this type included T cells, cytotoxic T cells, macrophages and a small number of B cells. The third type of vasculopathy was characterized by fibrinoid material deposition and cellular infiltration in the arterial neointima with immunoglobulin and complement deposition and infiltration of T cells, macrophages and polymorphonuclear leukocytes (Figure 7Q–T), suggesting both chronic humoral and cellular rejection-associated vasculopathy. The final type of vasculopathy was characterized by the narrowing of arteries with a fibrotic neointima, but without fibrinoid material or cellular infiltration (Figure 6). Before the development of fibrosis in the thickening neointima, fibrin exudation and/or cell infiltration was usually seen in the arteries (Figure 3). This type of vasculopathy, therefore, termed fully developed vasculopathy, may be the end result of humoral rejection-associated and/or cellular rejection-associated vasculopathy. In graftectomy samples from the gradually weakened group between days 78 and 179, fully developed and chronic humoral rejection-associated vasculopathy was common (Figure 6). Evidence of chronic cellular rejection-associated vasculopathy or a combination of both chronic humoral and cellular rejection-associated vasculopathy was present in a limited number of arteries.

Discussion

The production of GalT-KO swine may represent a critical step toward the clinical reality of solid organ xenotransplantation (2,11,12,20). In the present study of GalT-KO heart xenografts transplanted into baboons, HAR was prevented and graft survival improved over previous reports, even without the adsorption of anti-Gal antibodies or the continuous inhibition of complement (11–15). Furthermore, one GalT-KO graft survived for almost 6 months after transplantation. We consider these results very encouraging. However, all GalT-KO heart grafts underwent graft failure, despite chronic immunosuppression. The present study characterizes the pathology associated with AHXR, ACXR and chronic rejection in GalT-KO xenografts in nonhuman primates.

The availability of GalT-KO pigs eliminated the anti-Gal antibody–Gal antigen interaction that was the major barrier to successful xenotransplantation in pig-to-nonhuman primate models (13,21–23). This intervention did not, however, eliminate the thrombotic microangiopathy that is characteristic of AHXR (24). Indeed, in the present study, AHXR, as characterized by thrombotic microangiopathy, developed in all the eight grafts. Non-Gal antibodies likely play an important role in the pathogenesis of AHXR and graft failure in xenogeneic transplants, as suggested by this study and several other recent reports (25,26).

Troponin T is a clinically valuable marker of myocardial injury in heart grafts (27), and we used it as an indicator of myocardial injury in this study. Increases in troponin T, particularly if sustained, were associated with thrombotic microangiopathy (AHXR) and progressively weaker contractions of the grafts. However, some animals demonstrated a discrepancy between troponin T levels and graft contractions. B223 showed a sudden increase and rapid recovery of troponin T around day 55, without an associated change in the beating of the graft. This troponin T leak may have been due to a localized myocardial infarction that may have been the result of an AHXR-mediated thrombus in a small myocardial artery. In contrast, B229 lost the graft in the absence of any rise of troponin T. Instead of necrosis of cardiomyocytes, which is associated with the release of troponin T, this animal might have lost its graft due to apoptotic myocardial injury that was mediated by the chronic, mild but persistent ischemic injury caused by the gradual development of AHXR.

The characterization of cellular rejection in vascularized xenograft models is still limited by the rapid development of AHXR. Initial studies in rodents concluded that graft-infiltrating cells consisted primarily of macrophages and NK cells, and, in view of the small number of T cells in the infiltrates, that these responses were T cell independent (28,29). In the present study, however, the cellular response to discordant xenografts was characterized by an infiltration of $CD3^+$ T cells, $CD4^+$ cells, $CD8^+$ cells and $CD68^+$ macrophages. $CD3^+$ T cells infiltrated early after transplantation. Many CD3 and TIA-1^+ cytotoxic T cells were present in the infiltrate as were a small number of NK cells. These findings suggest that T-cell-dependent immunologic pathways play a significant role in xenograft rejection. Although *in vitro* assays showed general unresponsiveness of recipients to pig and baboon stimulators in MLR and circulating antipig IgM and IgG were undetectable by FACS (11,12), probably because of continuous immunosuppression, the T-cell infiltrates and IgG deposition seen in the grafts suggest that T cells were involved in the rejection. Several studies of human antipig cellular xenoreactivity support our findings; they have demonstrated a strong human antipig cell-mediated cytotoxic response that involves $CD8^+$ and/or $CD4^+$ cells, and have implicated $CD4^+$ cells as important mediators of macrophages, T-cell and B-cell activation (30–35). Therefore, as in allotransplantation, T cells may function as an initiating factor in the immune response to the xenografts and may contribute to the development of not only ACXR but also AHXR, through both direct and indirect pathways of immune recognition. In the present study, similar numbers of $CD4^+$ and $CD8^+$ T cells infiltrated the grafts, although $CD8^+$ T cells predominate in allograft rejection, suggesting a strong role for class II-restricted T-cell-mediated reactions in ACXR. In our results, three grafts in the gradually weakened group developed interstitial mononuclear cell infiltrates, as is characteristic of ACXR. In particular, in B223, the number of cell infiltrates increased significantly as the level of MMF was decreased (see Figure 5). On the other hand, two grafts in the rapidly weakened group had cellular infiltrates comprising neutrophils and macrophages as well as CD3+ T cells, suggesting that the humoral and T-cell responses developed together. The importance of T-cell immunity in xenotransplantation may be often underestimated because humoral immunity often masks T-cell immunity and obscures the pathological findings of ACXR in xenotransplantation. As is now the case in allotransplantation, ACXR may eventually become a more important and common type of xenograft rejection.

In clinical heart transplantation, CAV is the leading obstacle to long-term graft survival (36,37). It is widely established that CAV in allografts is caused by a combination of chronic immune and nonimmune injury, and that the immune mechanism involves both cellular rejection (endoarteritis or endothelialitis) in arteries and humoral rejection by circulating antidonor antibodies (36,37). NK cells might also have pathogenetic significance (38).

The development of chronic xenograft vasculopathy, which is considered to be a characteristic feature of chronic xenograft rejection, was previously reported in a small

number of hearts transplanted from pigs transgenic for hDAF or CD46 to primates (14,15,23). However, the pathogenic mechanism of the development of chronic xenograft vasculopathy has not been clearly determined. In the present study, chronic xenograft vasculopathy developed in the three grafts from the gradually weakened group between 78 and 179 days following transplantation. We recognized four major manifestations of chronic xenograft vasculopathy based on their histologic appearance: (1) chronic humoral rejection-associated vasculopathy, (2) chronic cellular rejection-associated vasculopathy, (3) both chronic humoral and cellular rejection-associated vasculopathy and (4) fully developed vasculopathy, which may be the end result of humoral rejection-associated and/or cellular rejection-associated vasculopathy. These histological findings suggest that prolonged antibody- and/or cell-mediated rejection can induce chronic xenograft vasculopathy. In the present study, chronic humoral rejection-associated vasculopathy was more frequently seen in the grafts than chronic cellular rejection, suggesting that chronic humoral rejection is likely the dominant mechanism for the development of chronic xenograft vasculopathy in this model.

Clinical application of xenotransplantation first requires the demonstration of efficacy in a nonhuman primate model. The ISHLT has suggested as a reasonable standard 60% graft survival of life-supporting orthotopic pig hearts in primates at 90 days (39). The FDA Advisory Subcommittee on Xenotransplantation has a similar recommendation of a median survival of 90 days in the orthotopic position as a possible standard for clinical application (40). In the present study, median and longest survivals of heterotopic hearts in a baboon were 78 (exclusion of euthanized animals) and 179 days, respectively. Future studies aimed at preventing acute and chronic antibody- and cell-mediated rejection in xenografts from GalT-KO donors are warranted.

In the present study, the response to GalT-KO cardiac xenografts in baboons was not controlled by our chronic immunosuppressive protocols, and acute and chronic humoral and cellular rejection developed in the grafts. We believe that improved strategies for inducing xenogeneic T-cell tolerance and preventing acute and chronic humoral and cell-mediated graft rejection may be required for long-term xenograft survival. Ongoing studies at our center are aimed at the induction of immunological tolerance to miniature swine organs in nonhuman primates by chimerism induction (41) and donor vascularized thymus grafting (20).

Acknowledgments

The authors thank Ms. Emma Samelson-Jones for her special support in editing the manuscript. The authors would also like to thank Novartis Pharma AG (Basel, Switzerland) for generously providing anti-CD 154 mAb and Immerge BioTherapeutics, Inc. (Cambridge, MA) for the supply of LoCD2b mAb and cobra venom factor. This work was supported in part by NIH Program Project 1PO1 A145897 and by a Sponsored Research Agreement between Immerge BioTherapeutics, Inc. and the Massachusetts General Hospital. F.J.M.F.D. was a recipient of grants from the Ter Meulen Fund from the Royal Netherlands Academy of Arts and Sciences, the Prof Michael-van Vloten Fund and the Netherland-America Foundation. A.S. was a recipient of a grant from the Japanese Society for the Promotion of Science, grant-in-aid for scientific research (CI8591787; C20591900)

References

1. Sachs DH, Sykes M, Robson SC, Cooper DK. Xenotransplantation. Adv Immunol. 2001; 79:129–223. [PubMed: 11680007]
2. Cooper DK. Clinical xenotransplantion—how close are we? Lancet. 2003; 362:557–559. [PubMed: 12932390]
3. Cooper DK, Gollackner B, Sachs DH. Will the pig solve the transplantation backlog? Annu Rev Med. 2002; 53:133–147. [PubMed: 11818467]

4. Bach FH, Robson SC, Winkler H, et al. Barriers to xenotransplantation. Nat Med. 1995; 1:869–873. [PubMed: 7585204]
5. Platt JL. The immunological barriers to xenotransplantation. Crit Rev Immunol. 1996; 16:331–358. [PubMed: 8954254]
6. Good AH, Cooper DK, Malcolm AJ, et al. Identification of carbohydrate structures that bind human antiporcine antibodies: Implications for discordant xenografting in humans. Transplant Proc. 1992; 24:559–562. [PubMed: 1566430]
7. Alwayn IP, Basker M, Buhler L, Cooper DK. The problem of anti-pig antibodies in pig-to-primate xenografting: Current and novel methods of depletion and/or suppression of production of anti-pig antibodies. Xenotransplantation. 1999; 6:157–168. [PubMed: 10503781]
8. Logan JS. Prospects for xenotransplantation. Curr Opin Immunol. 2000; 12:563–568. [PubMed: 11007360]
9. Phelps CJ, Koike C, Vaught TD, et al. Production of alpha-1,3-galactosyltransferase-deficient pigs. Science. 2003; 299:411–414. [PubMed: 12493821]
10. Kolber-Simonds D, Lai L, Watt SR, et al. Production of alpha-1,3-galactosyltransferase null pigs by means of nuclear transfer with fibroblasts bearing loss of heterozygosity mutations. Proc Natl Acad Sci USA. 2004; 101:7335–7340. [PubMed: 15123792]
11. Kuwaki K, Tseng YL, Dor FJ, et al. Heart transplantation in baboons using alpha 1,3-galactosyltransferase gene-knockout pigs as donors: Initial experience. Nat Med. 2005; 11:29–31. [PubMed: 15619628]
12. Tseng YL, Kuwaki K, Dor FJ, et al. Alpha 1,3-galactosyltransferase gene-knockout pig heart transplantation in baboons with survival approaching 6 months. Transplantation. 2005; 80:1493–1500. [PubMed: 16340796]
13. Kozlowski T, Shimizu A, Lambrigts D, et al. Porcine kidney and heart transplantation in baboons undergoing a tolerance induction regimen and antibody adsorption. Transplantation. 1999; 67:18–30. [PubMed: 9921791]
14. Kuwaki K, Knosalla C, Dor FJ, et al. Suppression of natural and elicited antibodies in pig-to-baboon heart transplantation using a human anti-human CD154 mAb-based regimen. Am J Transplant. 2004; 4:363–372. [PubMed: 14961988]
15. Houser SL, Kuwaki K, Knosalla C, et al. Thrombotic microangiopathy and graft arteriopathy in pig hearts following transplantation into baboons. Xenotransplantation. 2004; 11:416–425. [PubMed: 15303978]
16. Stewart S, Winters GL, Fishbein MC, et al. Revision of the 1990 working formulation for the standardization of nomenclature in the diagnosis of heart rejection. J Heart Lung Transplant. 2005; 24:1710–1720. [PubMed: 16297770]
17. Shimizu A, Yamada K, Yamamoto S, et al. Thrombotic microangiopathic glomerulopathy in hDAF-transgenic swine-to-baboon kidney xenografts. J Am Soc Nephrol. 2005; 16:2732–2745. [PubMed: 16049072]
18. Shimizu A, Meehan SM, Kozlowski T, et al. Acute humoral xenograft rejection: Destruction of the microvascular capillary endothelium in pig-to-nonhuman primate renal grafts. Lab Invest. 2000; 80:815–830. [PubMed: 10879733]
19. Madsen JC, Sachs DH, Fallon JT, Weissman NJ. Cardiac allograft vasculopathy in partially inbred miniature swine: I. Time course, pathology, and dependence on immune mechanisms. J Thorac Cardiovasc Surg. 1996; 111:1230–1239. [PubMed: 8642825]
20. Yamada K, Yazawa K, Shimizu A, et al. Marked prolongation of porcine renal xenograft survival in baboons through the use of alpha 1,3-galactosyltransferase gene-knockout donors and the co-transplantation of vascularized thymic tissue. Nat Med. 2005; 11:32–34. [PubMed: 15619627]
21. Cozzi E, White DJ. The generation of transgenic pigs as potential organ donors for humans. Nat Med. 1995; 1:964–966. [PubMed: 7585226]
22. Lambrigts D, Sachs DH, Cooper DK. Discordant organ xenotransplantation in primates: World experience and current status. Transplantation. 1998; 66:547–561. [PubMed: 9753331]
23. McGregor CG, Teotia SS, Byrne GW, et al. Cardiac xenotransplantation: Progress toward the clinic. Transplantation. 2004; 78:1569–1575. [PubMed: 15591943]

24. Shimizu A, Hisashi Y, Kuwaki K, et al. Thrombotic microangiopathy associated with humoral rejection of cardiac xenografts from alpha 1,3-galactosyltransferase gene-knockout pigs in baboons. Am J Pathol. 2008; 172:1471–1481. [PubMed: 18467706]
25. Lam TT, Paniagua R, Shivaram G, et al. Anti-non-Gal porcine endothelial cell antibodies in acute humoral xenograft rejection of hDAF-transgenic porcine hearts in cynomolgus monkeys. Xenotransplantation. 2004; 11:531–535. [PubMed: 15479463]
26. Chen G, Qian H, Starzl T, et al. Acute rejection is associated with antibodies to non-Gal antigens in baboons using Gal-knockout pig kidneys. Nat Med. 2005; 11:1295–1298. [PubMed: 16311604]
27. Kuwaki K, Knosalla C, Dor FJMF, et al. Troponin T levels in baboons with pig heterotopic heart transplants. J Heart Lung Transplant. 2005; 24:92–94. [PubMed: 15653386]
28. Candinas D, Belliveau S, Koyamada N, et al. T cell independence of macrophage and natural killer cell infiltration, cytokine production, and endothelial activation during delayed xenograft rejection. Transplantation. 1996; 62:1920–1927. [PubMed: 8990388]
29. Seebach JD, Waneck GL. Natural killer cells in xenotransplantation. Xenotransplantation. 1997; 4:201–211.
30. Yamada K, Seebach J, DerSimonian H, Sachs DH. Human anti-pig T-cell mediated cytotoxity. Xenotransplantation. 1996; 3:179–187.
31. Shishido S, Naziruddin B, Xu XC, et al. Indirect recognition of porcine xenoantigens by human CD4+ T cell clones. Transplantation. 1998; 65:706–712. [PubMed: 9521207]
32. Friedman T, Shimizu A, Smith RN, et al. Human CD4+ T cells mediate rejection of porcine xenografts. J Immunol. 1999; 162:5256–5262. [PubMed: 10228000]
33. Sebille F, Dorling A, Lechler RI. The cellular rejection of xenografts—recent insights. Xenotransplantation. 2003; 10:4–6. [PubMed: 12535219]
34. Cowan PJ, Aminian A, Barlow H, et al. Renal xenografts from triple-transgenic pigs are not hyperacutely rejected but cause coagulopathy in non-immunosuppressed baboons. Transplantation. 2000; 69:2504–2515. [PubMed: 10910270]
35. Davila E, Byrne GW, LaBreche PT, et al. T-cell responses during pig-to-primate xenotransplantation. Xenotransplantation. 2006; 13:31–40. [PubMed: 16497210]
36. Cotts WG, Johnson MR. The challenge of rejection and cardiac allograft vasculopathy. Heart Fail Rev. 2001; 6:227–240. [PubMed: 11391041]
37. Soleimani B, Lechler RI, Hornick PI, George AJ. Role of alloantibodies in the pathogenesis of graft arteriosclerosis in cardiac transplantation. Am J Transplant. 2006; 6:1781–1785. [PubMed: 16771817]
38. Uehara S, Chase CM, Kitchens WH, et al. NK cells can trigger allograft vasculopathy: The role of hybrid resistance in solid organ allografts. J Immunol. 2005; 175:3424–3430. [PubMed: 16116237]
39. Cooper DK, Keogh AM, Brink J, et al. Xenotransplantation Advisory Committee of the International Society for Heart and Lung Transplantation. Report of the Xenotransplantation Advisory Committee of the International Society for Heart and Lung Transplantation: The present status of xenotransplantation and its potential role in the treatment of end-stage cardiac and pulmonary diseases. J Heart Lung Transplant. 2000; 19:1125–1165. [PubMed: 11124485]
40. U.S. Department of Health and Human Services, FDA, Center for Biologics Evaluation and Research. Draft Report of the Biological Response Modifiers Advisory Subcommittee on Xenotransplantation; Bethesda, MD. 1999.
41. Tseng YL, Sachs DH, Cooper DK. Porcine hematopoietic progenitor cell transplantation in nonhuman primates: A review of progress. Transplantation. 2005; 79:1–9. [PubMed: 15714161]

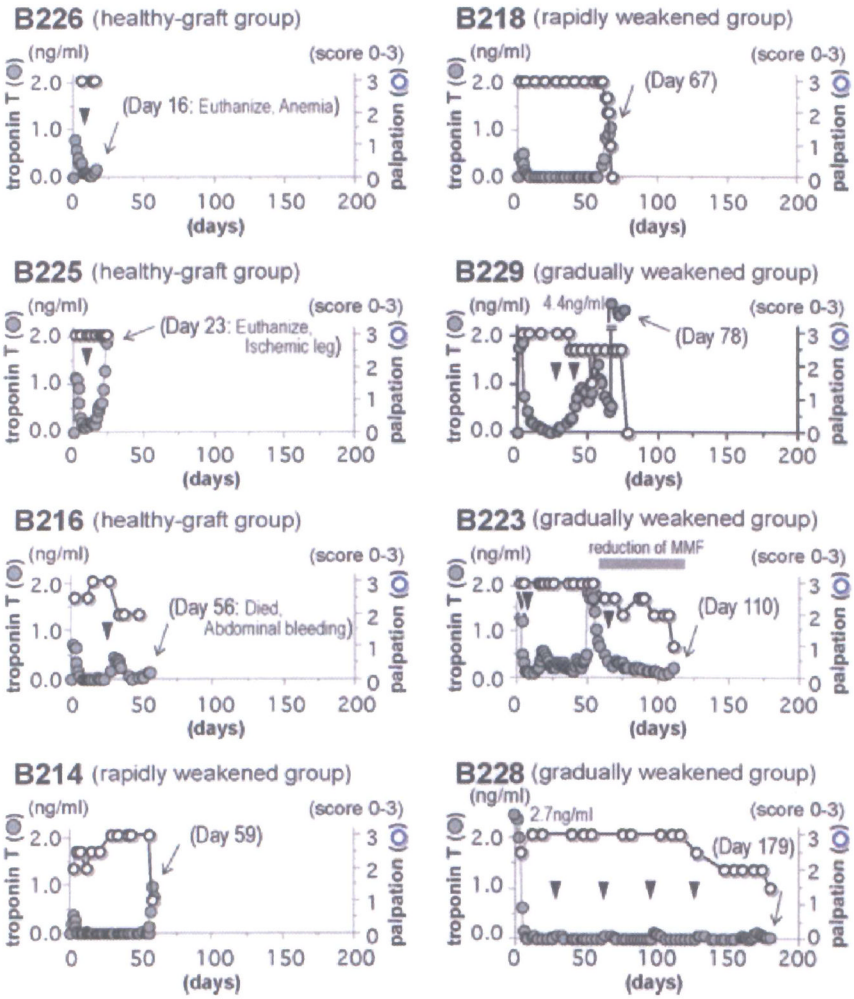

Figure 1. Serum troponin T levels in recipients and palpation scores based on the strength of contraction of cardiac xenografts

Normal troponin T levels are less than 0.10 ng/mL. Contraction of grafts was monitored by palpation and scored 0–3. The arrowheads indicate the day of biopsies and the arrow indicates the day of graftectomy. The eight heterotopic cardiac grafts were divided into the three groups based on their rejection profile: (1) healthy-graft group (B226, B225 and B216), (2) rapidly weakened group (B214 and B218) and (3) gradually weakened group (B229, B223 and B228). B226 and B225 were euthanized and B216 died with beating heart grafts, as a result of anemia (during a period when no donor blood was available), ischemia in a leg (associated with an indwelling femoral artery catheter) or spontaneous intra-abdominal hemorrhage, on day 23, 16 or 56, respectively.

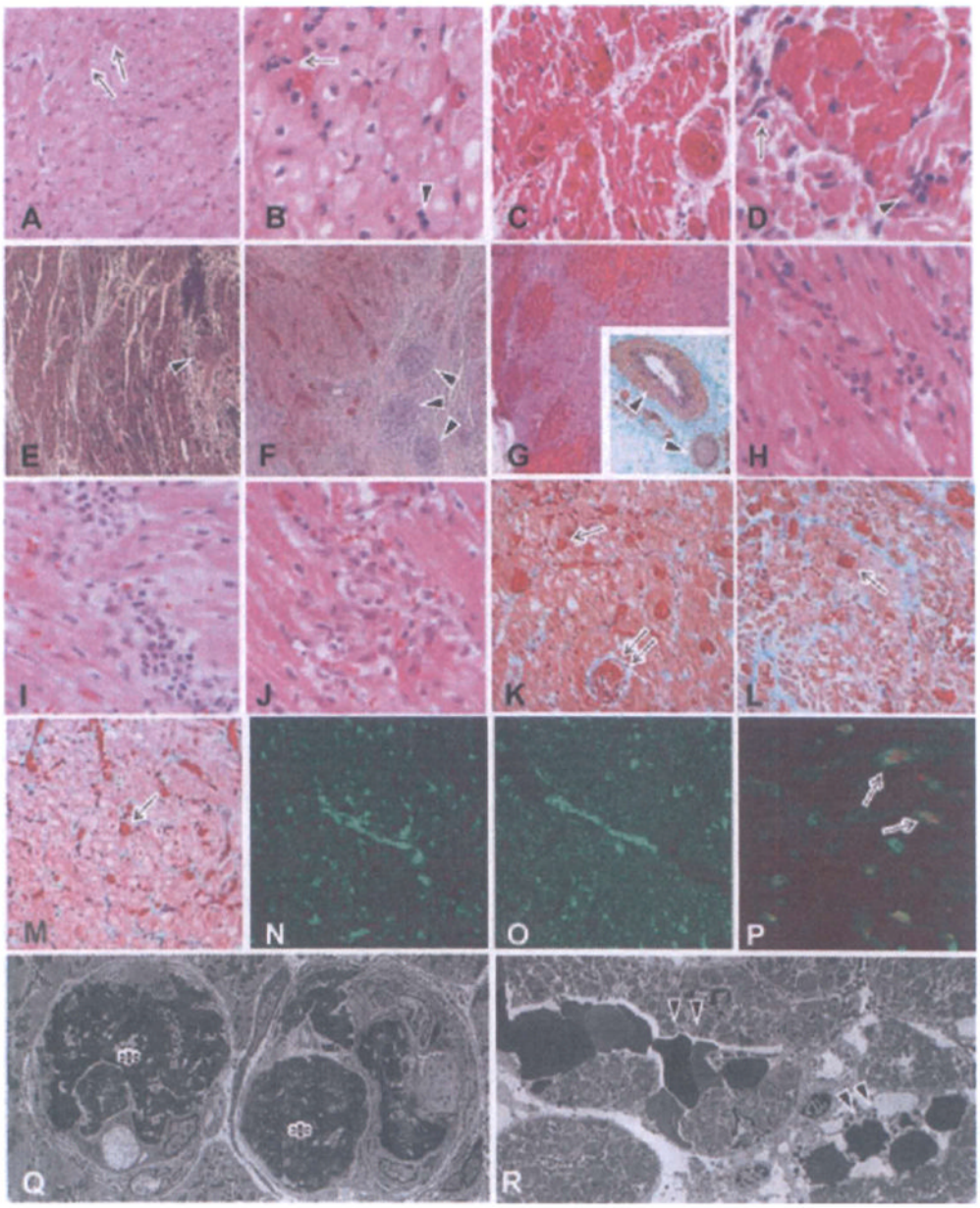

Figure 2. Histological features of grafts showing the development of acute humoral xenograft rejection (AHXR), acute cellular xenograft rejection (ACXR) and chronic xenograft rejection

In graftectomy samples from B226 (A, B:day 16, HE stain), thrombi (arrows in A) were seen in capillaries. Polymorphonuclear leukocytes (arrow in B) and mononuclear cells (arrowhead in B) infiltrated the grafts. In graftectomy samples from B214 (C, D: day 59, HE stain), interstitial hemorrhage and multiple microthrombi in the microvasculature developed. In addition to the infiltration of polymorphonuclear leukocytes (arrow in D), focal mononuclear cells (arrowhead in D) infiltrated the graft. In graftectomy samples from B229 (E, H, K: day 78), B223 (F, I, L, N–P: day 110) and B228 (G, J, M: day 179) (E–J: HE stain; inset in G, K–M: EMG stain), multiple microthrombi, an irregular distribution of interstitial hemorrhage and chronic xenograft vasculopathy (arrowheads in E–G) developed along with a focal mononuclear cell infiltrate (H–J). AHXR was characterized by thrombotic microangiopathy with multiple microthrombi in capillaries (arrows in K–M) and arteries

(double arrow in K) in the grafts, and by immunoglobulin and complement deposition (N: IgM; 0: C5b-9). Two-color immunostaining for CD41 (red color) and C4d (green color) showed that almost all of the $CD41^+$ thrombi (arrows in P) were detected within vessels that contained deposits of complement. Electron microscopy (Q, R) revealed damaged capillaries in the graft of B228 on day 179 (× 1900). The damage was characterized by the loss of endothelial cells with fibrin thrombi (asterisks in Q) and capillary destruction (arrowheads in R) with interstitial hemorrhage.

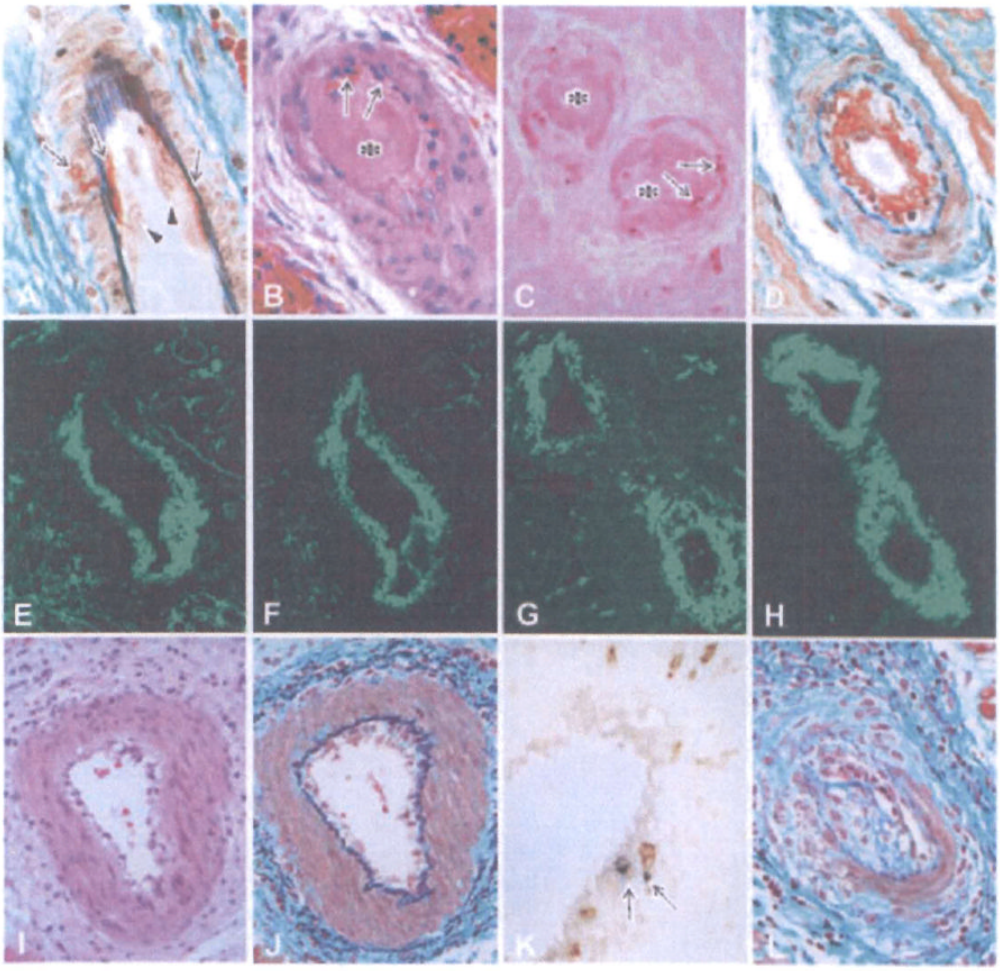

Figure 3. Histological features of cardiac grafts showing fibrinoid necrosis and endothelialitis in the arteries

The early fibrinoid necrosis in arteries (A: B214, day 59, EMG stain) showed enlarged endothelial cells (arrowheads) and the exudation of fibrinoid materials (arrows). In advanced AHXR (B–D: B218, day 67; B: HE stain, C: TUNEL stain, D: EMG stain), arteries showed fibrinoid necrosis with thrombus formation (asterisks in B and C), neutrophil infiltration (arrows in B), $TUNEL^+$ cells (arrows in C) and deposits of fibrin (D, E), immunoglobulin (F: IgM) and complement (G: C4d), along with neointimal thickening (D). Two-color immunostaining (H) for CD41 (red color) and C4d (green color) showed that $CD41^+$ thrombi were detected within small arteries that contained deposits of complement. Endothelialitis (I) was noted in arteries with infiltration of mononuclear cells underneath the endothelium (J) and media (J), infiltration of both CD3 and $TIA\text{-}1^+$ cytotoxic T cells (arrows in K), and neointimal thickening (L) (I–L: B228, day 179; I, J, L: EMG stain, K: two-color stain with CD3 (brown) and TIA-1 (blue)).

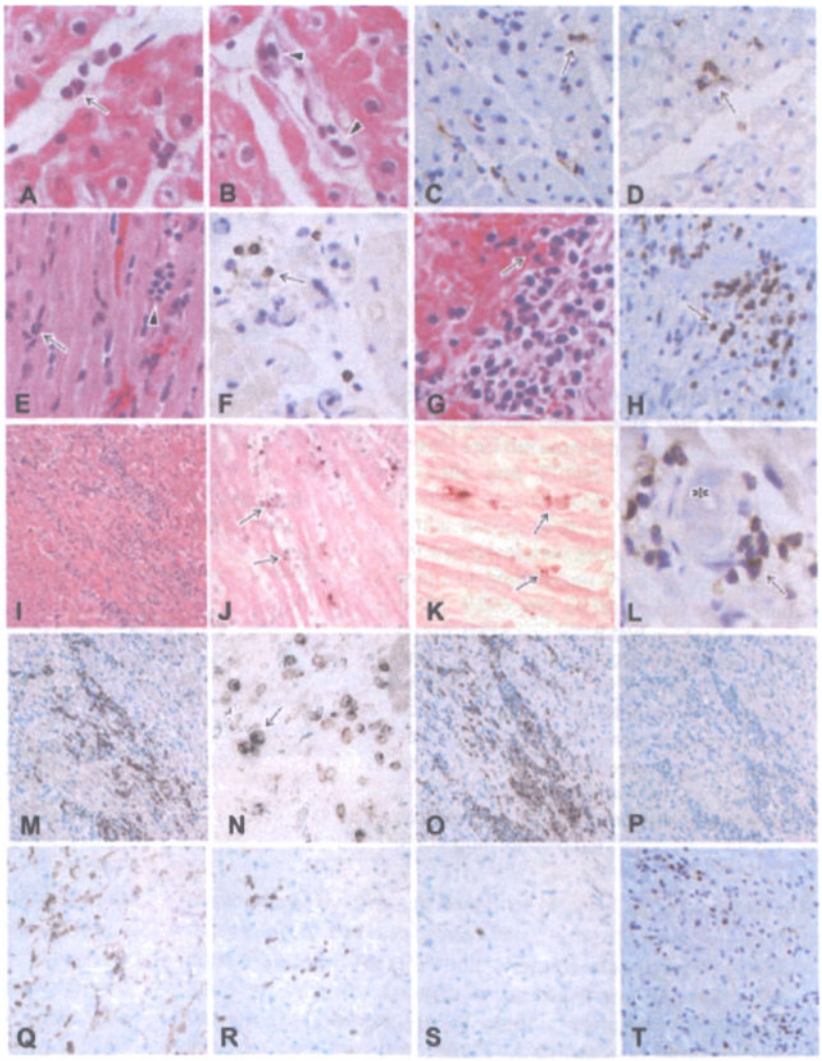

Figure 4. Histological features of grafts showing graft infiltrating cells and the development of acute cellular xenograft rejection (ACXR)

Polymorphonuclear leukocytes (arrow in A), mononuclear cells (arrowheads in B), $CD68^+$ macrophages (arrow in C) and a small number of $CD3^+$ cells (arrow in D) infiltrated the graft 7 days after transplantation. In the healthy-graft group (E, F: B216, day 56; E: HE stain, F: CD3 stain), polymorphonuclear leukocytes (arrow in E) and mononuclear cells (arrowhead in E), including a small number of $CD3^+$ cells (arrow in F), infiltrated the grafts. In rapidly weakened group (G, H: B218, day 67; G: HE stain, H: CD3 stain) and gradually weakened group (I: B223, day 110, HE stain), focal mononuclear cell infiltration was evident in the graft, showing ACXR. Some $TUNEL^+$ dead cells (arrows in J, K) were seen in contact with infiltrating mononuclear cells (J, K: B223, day 110, TUNEL stain). Some thrombi (asterisk in L) were present with $CD3^+$ cell infiltration (arrow) (L: B223, day 110, CD3 stain). The phenotypes of the infiltrating cells included many $CD3^+$ T cells (H, M, T), both TIA-1 and $CD3^+$ cytotoxic T cells (N), $CD68^+$ macrophages (O), $CD4^+$ cells (Q), $CD8^+$ cells (R) and a small number of $CD20^+$ B cells (P) and $NKB\text{-}1^+$ NK cells (S) (M–P: B223, day 110, Q–T: B229, day 179; M, T: CD3 stain, N: two-color stain with CD3 (brown) and TIA-1 (blue), O: CD68 stain, P: CD20 stain, Q: CD4 stain, R: CD8 stain, S: NKB-1 stain).

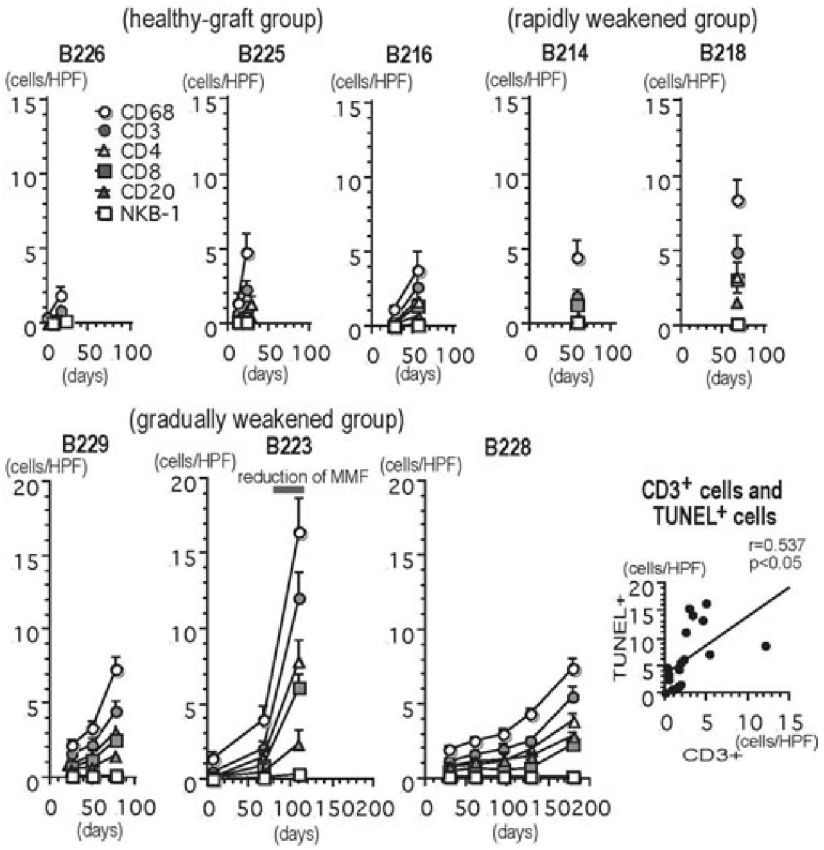

Figure 5. The number of infiltrating cells in the grafts (cells/single field of 0.0625 mm^2) and the correlation between CD3$^+$ T cells and TUNEL$^+$ dead cells

The number of infiltrating cells of all phenotypes except NKB-1$^+$ cells increased after transplantation and during the development of graft failure (healthy-graft group: B226, B225 and B216; rapidly weakened group: B214 and B218 and gradually weakened group: B229, B223 and B228). The results are depicted as the mean ± standard error, as calculated from 40 randomly selected fields. There was a statistically significant correlation between the number of CD3$^+$ T cells and the number of TUNEL$^+$ dead cells in capillaries and the interstitium in the grafts ($p < 0.05$).

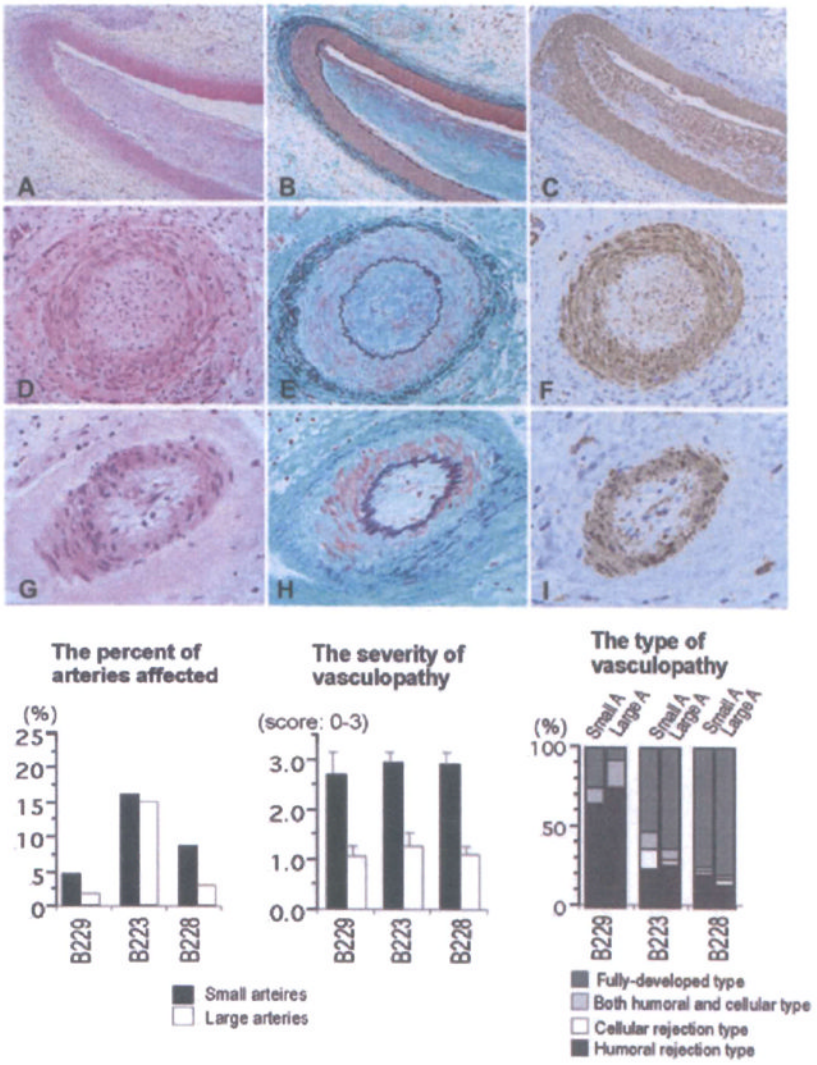

Figure 6. Histological features of grafts showing chronic xenograft vasculopathy (A–I: B223, day 110; A, D, G: HE stain, B, E, F: EMG stain, C, F, I: α-actin stain)

Chronic xenograft vasculopathy in arteries was characterized by the narrowing of the arterial lumen with intimal fibrous thickening consisting of α-actin$^+$ cells without elastosis. Neither fibrinoid material nor cellular infiltration was seen in arteries, suggesting fully developed vasculopathy. The distribution of chronic vasculopathy in grafts, including the percent of arteries affected, as well as the severity and types of chronic vasculopathy is also shown. Although a similar percentage of small and large arteries were affected by chronic xenograft vasculopathy, the vasculopathy was, on average, more severe in the smaller arteries. Large number of arteries that showed evidence of vasculopathy also had fully developed or humoral-associated rejection types.

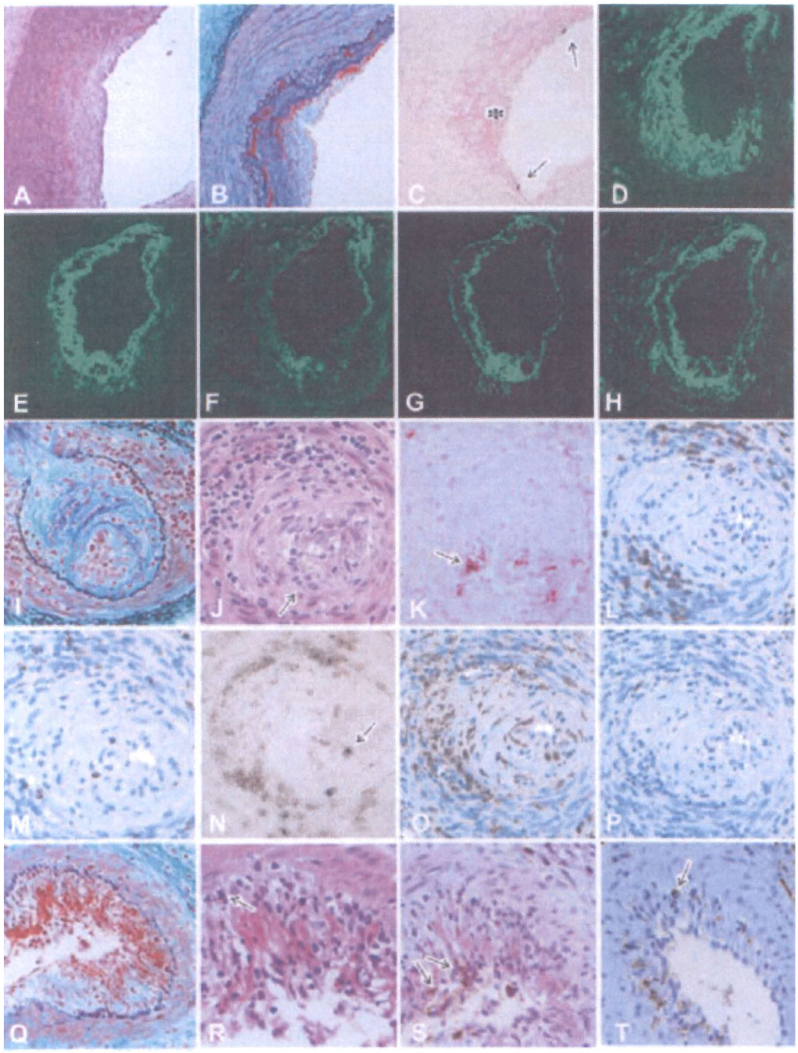

Figure 7. Histological features of chronic xenograft vasculopathy

In chronic humoral rejection-associated vasculopathy (A–H: B229, day 78), fibrinoid materials were present within a thickened intima (A: HE stain, B: EMG stain). TUNEL$^+$ dead cells (arrows in C), that may be endothelial cells, were detected on the luminal surface of arteries along with exudative lesions (asterisk in C) (C: TUNEL method). The deposition of fibrin (D), IgM (E), IgG (F), C4d (G) and C5b-9 (H) was detected in arteries. Chronic cellular rejection-associated vasculopathy (I–P: B223, day 110) was characterized by active endothelialitis (arrow in J), presence of TUNEL$^+$ dead cells (arrow in K) and cellular infiltration in the arterial intima (I: EMG stain, J: HE stain, K: TUNEL method). Cellular infiltrate in arterial walls was composed of T cells (L: CD3 stain), cytotoxic cells (M: TIA-1 stain), both CD3 and TIA-1$^+$ cytotoxic T cells (N: two-color stain with CD3 (brown) and TIA-1 (blue)), macrophages (O: CD68 stain) and a small number of B cells (P: CD20 stain). Both chronic humoral and cellular rejection-associated vasculopathy (Q–T: B223, day 110) was characterized by fibrinoid material deposition and cellular infiltration in arterial intima (Q: EMG stain). Cellular infiltrate in the intima was composed of polymorphonuclear leukocytes (arrow in R), T cells (arrows in S) and macrophages (arrow in T) (R: HE stain, S: CD3 stain, T: CD68 stain).

Table 1

The deposition of immunoglobulin and complement in the GalT-KO heart grafts

Animal ID and day of Bx or Gx	IgM	IgG	C3	C4d	C5b-9	Microthrombi
B226 (healthy-graft group)						
POD 0	(1+)	(−)	(−)	(−)	(−)	(−)
POD 16	(2+)	(1+)	(1+)	(2+)	(−)	(1+)
B225 (healthy-graft group)						
POD 13	(1+)	(−)	(1+)	(1+)	(1+)	(1+)
POD 23	(2+)	(1+)	(1+)	(2+)	(1+)	(1+)
B216 (healthy-graft group)						
POD 27	(1+)	(−)	(−)	(1+)	(1+)	(1+)
POD 56	(2+)	(1+)	(1+)	(2+)	(1+)	(2+)
B214 (rapidly weakened group)						
POD 59	*1*	*1*	*1*	(2+)*1*	*1*	(2+)
B218 (rapidly weakened group)						
POD 67	(3+)	(2+)	(2+)	(3+)	(2+)	(3+)
B229 (gradually weakened group)						
POD 27	(1+)	(−)	(1+)	(1+)	(1+)	(1+)
POD 50	(2+)	(−)	(2+)	(2+)	(2+)	(1+)
POD 78	(3+)	(2+)	(2+)	(3+)	(2+)	(2+)
B223 (gradually weakened group)						
POD 0	(1+)	(−)	(−)	(−)	(−)	(−)
POD 7	(2+)	(−)	(1+)	(1+)	(1+)	(1+)
POD 68	(2+)	(1+)	(2+)	(2+)	(2+)	(1+)
POD 110	(3+)	(2+)	(2+)	(3+)	(2+)	(3+)
B228 (gradually weakened group)						
POD 27	(1+)	(−)	(1+)	(1+)	(−)	(1+)
POD 62	(1+)	(−)	(1+)	(1+)	(1+)	(1+)
POD 95	(1+)	(−)	(1+)	(1+)	(1+)	(1+)
POD 127	(2+)	(1+)	(2+)	(2+)	(2+)	(1+)
POD 179	(3+)	(2+)	(2+)	(2+)	(2+)	(2+)

Day of Bx or Gx = day of biopsies or graftectomy; POD = postoperative day.

The signal intensity and their distribution was divided into (−) to (3+).

[1] *C4d* was assessed using formalin-fixed paraffin-embedded samples, because the condition of frozen tissue is not enough to show a reliable interpretation.